Evaluation of Zirconium and Hafnium Complexes that Contain the Electron-Withdrawing Diamido/Donor Ligand $[(2,6\text{-}Cl_2C_6H_3NCH_2CH_2)_2NCH_3)]^{2-}$ for the Polymerization of 1-Hexene

Richard R. Schrock,* Jennifer Adamchuk, Klaus Ruhland, and L. Pia H. Lopez

Department of Chemistry, Massachusetts Institute of Technology, 77 Massachusetts Avenue, Cambridge, Massachusetts 02139

Received August 24, 2004

The triamine $(2,6\text{-}Cl_2C_6H_3NHCH_2CH_2)_2NMe$ ($H_2[Ar_{Cl}N_2NMe]$) can be prepared through the Pd-catalyzed coupling between 2-bromo-1,3-dichlorobenzene and $(H_2NCH_2CH_2)_2NH$ to give $(2,6\text{-}Cl_2C_6H_3NHCH_2CH_2)_2NH$, followed by methylation of the central nitrogen with MeI. Zirconium and hafnium complexes that were prepared include $[Ar_{Cl}N_2NMe]M(NMe_2)_2$ (M = Hf or Zr), $[Ar_{Cl}N_2NMe]MCl_2$, $[Ar_{Cl}N_2NMe]MMe_2$, $[Ar_{Cl}N_2NMe]HfCl(i\text{-}Bu)$, $[Ar_{Cl}N_2NMe]HfMe(i\text{-}Bu)$, and $[Ar_{Cl}N_2NMe]Hf(i\text{-}Bu)_2$. An X-ray crystal structure shows $[Ar_{Cl}N_2NMe]Hf(i\text{-}Bu)_2$ to be a square pyramid in which one of the isobutyl groups occupies the apical position. Activation of dimethyl species with $\{Ph_3C\}\{B(C_6F_5)_4\}$, $B(C_6F_5)_3$, or $\{PhNMe_2H\}\{B(C_6F_5)_4\}$ yielded $\{[Ar_{Cl}N_2NMe]MMe\}^+$ cations paired with $\{B(C_6F_5)_4\}^-$ or $\{MeB(C_6F_5)_3\}^-$ anions; these species are active for the polymerization of 1-hexene. Activation of $[Ar_{Cl}N_2NMe]Hf(i\text{-}Bu)_2$ with $\{Ph_3C\}\{B(C_6F_5)_4\}$ or $B(C_6F_5)_3$ produced $\{[Ar_{Cl}N_2NMe]Hf(i\text{-}Bu)\}\{B(C_6F_5)_4\}$ and $\{[Ar_{Cl}N_2NMe]Hf(i\text{-}Bu)\}\{HB(C_6F_5)_3\}$, which are also active for the polymerization of 1-hexene. Isobutene was found to insert slowly into the M−R bond of these initiators in a 1,2 manner and was oligomerized at high concentrations of isobutene. Activation of $[Ar_{Cl}N_2NMe]HfMe(i\text{-}Bu)$ with $B(C_6F_5)_3$ resulted in selective abstraction of a methyl group to generate 95% $\{[Ar_{Cl}N_2NMe]Hf(i\text{-}Bu)\}\{MeB(C_6F_5)_3\}$. The rate of consumption of 1-hexene followed a first-order dependence on 1-hexene (and hafnium or zirconium), and zirconium was faster than hafnium. Although poly[1-hexene] generated by the zirconium catalyst was characteristic of a living system, significant β-hydride elimination was observed in polymerizations by hafnium catalysts. The hafnium product of β-hydride elimination was observed to reinitiate the polymerization of 1-hexene. We conclude that by replacing the mesityl substituents in the analogous $[(MesitylN_2NMe]^{2-}$ ligand with $2,6\text{-}Cl_2C_6H_3$ groups, decomposition is attenuated significantly, although living behavior is observed for zirconium catalysts only.

Introduction

Since McConville's discovery of titanium and zirconium olefin polymerization catalysts that contain simple aryl-substituted diamido ligands,[1−4] interest in "non-metallocene" early transition metal olefin polymerization catalysts, as well as late metal catalysts (which often contain nitrogen donor ligands), has increased markedly.[5−8] We have focused on diamido/donor ligands, e.g., $[(t\text{-}BuN\text{-}o\text{-}C_6H_4)_2O]^{2-}$ or $[(MesitylNCH_2)_2C(CH_3)(2\text{-}C_5H_4N)]^{2-}$.[9−13] The most interesting feature of several systems that contain one of these ligands is the fact that 1-hexene can be polymerized in a living fashion and intermediates in that process examined using NMR methods. A number of polymerization catalysts have now been published that are living to a greater or lesser degree.[14] Living characteristics result largely from a reduced tendency for β-hydride elimination from (in the case of a terminal olefin) either a 1,2 insertion product or a 2,1 insertion product. For non-metallocene systems other than the diamido/donor systems explored in our laboratory, the reader should consult papers by McConville,[1−4] Sita,[15−18] Kol,[19−21] Coates,[7,14,22] Jeon,[23] Brookhart,[24,25]Mashima,[26] and Fujita.[27]

In contrast to cationic zirconium and hafnium alkyl complexes that contain the $[(MesitylNCH_2)_2C(CH_3)(2\text{-}$

(1) Scollard, J. D.; McConville, D. H. *J. Am. Chem. Soc.* **1996**, *118*, 10008.
(2) Guérin, F.; McConville, D. H.; Payne, N. C. *Organometallics* **1996**, *15*, 5085.
(3) Guérin, F.; McConville, D. H.; Vittal, J. J. *Organometallics* **1996**, *15*, 5586.
(4) Guérin, F.; McConville, D. H.; Vittal, J. J. *Orgaometallics* **1997**, *16*, 1491.
(5) Britovsek, G. J. P.; Gibson, V. C.; Wass, D. F. *Angew. Chem., Int. Ed.* **1999**, *38*, 428.
(6) Gibson, V. C.; Spitzmesser, S. K. *Chem. Rev.* **2003**, *103*, 283.
(7) Coates, G. W. *J. Chem. Soc., Dalton Trans.* **2002**, 467.
(8) Kempe, R. *Angew. Chem., Int. Ed.* **2000**, *39*, 468.
(9) Schrock, R. R.; Baumann, R.; Reid, S. M.; Goodman, J. T.; Stumpf, R.; Davis, W. M. *Organometallics* **1999**, *18*, 3649.
(10) Baumann, R.; Schrock, R. R. *J. Organomet. Chem.* **1998**, *557*, 69.
(11) Goodman, J. T.; Schrock, R. R. *Organometallics* **2001**, *20*, 5205.
(12) Schrock, R. R.; Casado, A. L.; Goodman, J. T.; Liang, L.-C.; Bonitatebus, P. J., Jr.; Davis, W. M. *Organometallics* **2000**, *19*, 5325.
(13) Schrodi, Y.; Schrock, R. R.; Bonitatebus, P. J., Jr. *Organometallics* **2001**, *20*, 3560.
(14) Coates, G. W.; Hustad, P. D.; Reinartz, S. *Angew. Chem., Int. Ed.* **2002**, *41*, 2236.

10.1021/om040113h CCC: $30.25
Publication on Web 02/04/2005

Scheme 1. Synthesis of $[Ar_{Cl}N_2NMe]MCl_2$ (M = Hf, Zr)

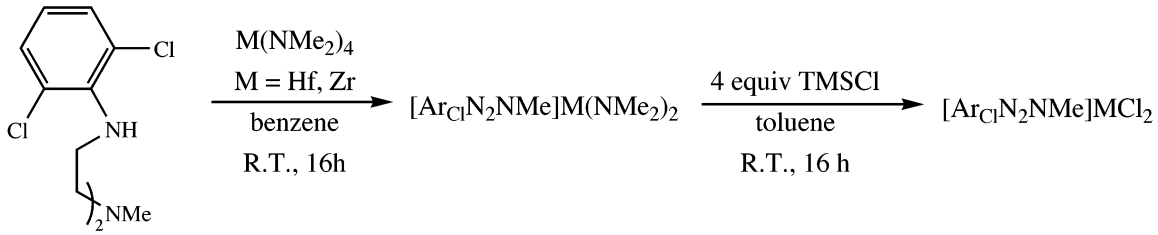

$C_5H_4N)]^{2-}$ ligand, cationic zirconium alkyl complexes that contain the $[(MesitylNCH_2CH_2)_2NMe]^{2-}$ ligand undergo ortho-methyl C−H activation during polymerization, which leads to formation of a catalytically inactive complex and therefore nonliving polymerization behavior.[13,28] This problem can be avoided through the use of 2,6-$Cl_2C_6H_3$ substituents instead of mesityl substituents.[28] Catalysts derived from this ligand appeared to be highly active for the polymerization of 1-hexene. In this paper we report the full investigation of zirconium and hafnium alkyl complexes that contain the $[(2,6\text{-}Cl_2C_6H_3NCH_2CH_2)_2NMe]^{2-}$ ligand. These results should be compared with a recent study of zirconium and hafnium catalysts that contain $[(2,6\text{-}X_2C_6H_3NCH_2)_2C(2\text{-}C_5H_4N)(CH_3)]^{2-}$ (X = Cl or F) ligands.[29]

Results

Preparation of $(2,6\text{-}Cl_2C_6H_3NHCH_2CH_2)_2NMe$ ($H_2[Ar_{Cl}N_2NMe]$) and Complexes that Contain the $[Ar_{Cl}N_2NMe]^{2-}$ Ligand. The palladium-catalyzed coupling reaction between 2-bromo-1,3-dichlorobenzene and $(H_2NCH_2CH_2)_2NH$ produces oily $H_2[(2,6\text{-}Cl_2C_6H_3NCH_2CH_2)_2NH]$ ($H_2[Ar_{Cl}N_2NH]$) in 75−85% yield. Impurities are present that we suspect result primarily from competitive coupling at the 2 and 6 positions. Ligand purification via column chromatography and recrystallization at this stage produced pure $H_2[Ar_{Cl}N_2NH]$ in 56% yield. The central nitrogen in $H_2[Ar_{Cl}N_2NH]$ was then methylated with MeI in the presence of K_2CO_3 in CH_3CN to give $H_2[Ar_{Cl}N_2NMe]$ in 63% yield.

$H_2[Ar_{Cl}N_2NMe]$ reacts smoothly with $M(NMe_2)_4$ (M = Hf, Zr) to give $[Ar_{Cl}N_2NMe]M(NMe_2)_2$ in 80−90% yield (Scheme 1).[28] The dimethylamido resonances in the proton NMR spectra of $[Ar_{Cl}N_2NMe]M(NMe_2)_2$ are found as two singlets, with the rest of the molecule having mirror symmetry in which the aryl groups rotate freely on the NMR time scale. The reaction of 3−5 equiv of TMSCl with $[Ar_{Cl}N_2NMe]M(NMe_2)_2$ affords $[Ar_{Cl}N_2NMe]MCl_2$, a molecule whose NMR spectra are also consistent with mirror symmetry. Alkylation of the $[Ar_{Cl}N_2NMe]MCl_2$ species with MeMgBr yields $[Ar_{Cl}N_2NMe]MMe_2$ complexes, which are white powders that are only sparingly soluble in toluene and bromobenzene. A single resonance for two methyl groups appears at 0.60 ppm in the room-temperature ^1H NMR spectrum of $[Ar_{Cl}N_2NMe]ZrMe_2$ in benzene-d_6, while two methyl resonances appear at 0.18 and 0.49 ppm in the spectrum of $[Ar_{Cl}N_2NMe]HfMe_2$. The two methyl resonances in the zirconium compound must be accidentally coincident, since in bromobenzene-d_5 two methyl resonances are found at 0.29 and 0.33 ppm in the ^1H NMR spectrum and two methyl resonances at 45.32 and 46.13 in the ^{13}C NMR spectrum.

On the basis of ^1H NOESY experiments the resonance for the MMe group closest to the NMe group is found downfield of the resonance for the other MMe group in the proton NMR spectrum. The MMe group nearest the NMe group will be called the Me_{syn} group, and that furthest from the NMe group will be called the Me_{anti} group. Although the resonance for the Me_{syn} group is found downfield of the resonance for the Me_{anti} group in the proton NMR spectrum, the resonance for the Me_{syn} group is found *up*field of the resonance for the Me_{anti} group in the *carbon* NMR spectrum.

Treatment of $[Ar_{Cl}N_2NMe]ZrCl_2$ with 2 equiv of isobutyllithium appeared to yield $[Ar_{Cl}N_2NMe]Zr(i\text{-}Bu)_2$, although this compound decomposed at room temperature and therefore could not be isolated. However, addition of 2 equiv of isobutyllithium to $[Ar_{Cl}N_2NMe]HfCl_2$ produced $[Ar_{Cl}N_2NMe]Hf(i\text{-}Bu)_2$ in 73% yield. Recrystallization of $[Ar_{Cl}N_2NMe]Hf(i\text{-}Bu)_2$ from pentane at −30 °C yielded single crystals suitable for X-ray diffraction (Figure 1). Crystal parameters can be found in Table 1 and bond lengths and angles in Table 2. The structure is approximately a square pyramid in which one of the isobutyl groups (C(5)) occupies the apical position in the square pyramid. The C(1)−Hf−N(3) bond angle is 139.59°, which is 9.17° greater than the analogous bond angle in $[Ar_{Cl}N_2NMe]ZrMe_2$;[28] the C(5)−Hf−N(3) angle therefore is only 118.79°, while the C(1)−Hf−C(5) angle is 101.62°. The Hf−N(3) bond distance of 2.378(3) Å is slightly shorter than the Hf−pyridyl bond distance of 2.416(9) Å in $[(2,6\text{-}Cl_2C_6H_3NHCH_2)_2C(CH_3)(2\text{-}C_5H_4N)]Hf(i\text{-}Bu)_2$,[29] but is still somewhat long for a donor−M distance in com-

(15) Jayaratne, K. C.; Sita, L. R. *J. Am. Chem. Soc.* **2000**, *122*, 958−959.
(16) Zhang, Y.; Keaton, R. J.; Sita, L. R. *J. Am. Chem. Soc.* **2003**, *125*, 9062.
(17) Keaton, R. J.; Jayaratne, K. C.; Henningsen, D. A.; Koterwas, L. A.; Sita, L. R. *J. Am. Chem. Soc.* **2001**, *123*, 6197−6198.
(18) Keaton, R. J.; Jayaratne, K. C.; Fettinger, J. C.; Sita, L. R. *J. Am. Chem. Soc.* **2000**, *122*, 12909.
(19) Tshuva, E. Y.; Goldberg, I.; Kol, M. *J. Am. Chem. Soc.* **2000**, *122*, 10706.
(20) Tshuva, E. Y.; Goldberg, I.; Kol, M.; Goldschmidt, Z. *Chem. Commun.* **2001**, 2120.
(21) Tshuva, E. Y.; Groysman, S.; Goldberg, I.; Kol, M.; Goldschmidt, Z. *Organometallics* **2002**, *21*, 662.
(22) Tian, J.; Hustad, P. D.; Coates, G. W. *J. Am. Chem. Soc.* **2001**, *123*, 5134.
(23) Jeon, Y.-M.; Park, S. J.; Heo, J.; Kim, K. *Organometallics* **1998**, *17*, 3161.
(24) Killian, C. M.; Tempel, D. J.; Johnson, L. K.; Brookhart, M. *J. Am. Chem. Soc.* **1996**, *118*, 11664.
(25) Brookhart, M.; Desimone, J. M.; Grant, B. E.; Tanner, M. J. *Macromolecules* **1995**, *28*, 5378.
(26) Mashima, K.; Fujikawa, S.; Tanaka, Y.; Urata, H.; Oshiki, T.; Tanaka, E.; Nakamura, A. *Organometallics* **1995**, *14*, 2633.
(27) Mitani, M.; Mohri, J.; Yoshida, Y.; Saito, J.; Ishii, S.; Tsuru, K.; Matsui, S.; Furuyama, R.; Nakano, T.; Tanaka, H.; Kojoh, S.; Matsugi, T.; Kashiwa, N.; Fujita, T. *J. Am. Chem. Soc.* **2002**, *124*, 3327.
(28) Schrock, R. R.; Bonitatebus, P. J., Jr.; Schrodi, Y. *Organometallics* **2001**, *20*, 1056.
(29) Schrock, R. R.; Adamchuk, J.; Ruhland, K.; Lopez, L. P. H. *Organometallics* **2003**, *22*, 5079.

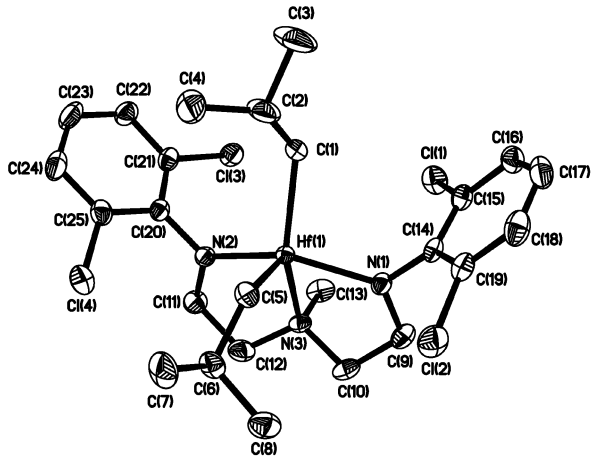

Figure 1. Thermal ellipsoid drawing of $[Ar_{Cl}N_2NMe]Hf(i\text{-}Bu)_2$ at the 30% probability level.

Table 1. Crystal Data and Structure Refinement for $[Ar_{Cl}N_2NMe]Hf(i\text{-}Bu)_2$

empirical formula	$C_{25}H_{35}Cl_4HfN_3$
fw	697.85
temperature	193(2) K
wavelength	0.71073 Å
cryst syst	monoclinic
space group	$P2_1/c$
unit cell dimens	$a = 11.0327(7)$ Å, $\alpha = 90°$ $b = 13.0463(9)$ Å, $\beta = 94.8850(10)°$ $c = 19.8936(13)$ Å, $\gamma = 90°$
volume	2853.0(3) Å^3
Z	4
density(calcd)	1.625 Mg/m^3
absorp coeff	4.049 mm^{-1}
$F(000)$	1384
cryst size	0.1 × 0.1 × 0.09 mm^3
θ range for data collection	1.85−28.29°
index ranges	$-8 \le h \le 14$, $-16 \le k$ 17, $-26 \le l \le 26$
no. of reflns collected	17 941
no. of indep reflns	6725 [R(int) = 0.0565]
completeness to $\theta = 28.29°$	94.7%
refinement method	full-matrix least-squares on F^2
no. of data/restraints/params	6725/0/304
goodness-of-fit on F^2	0.810
final R indices [$I > 2\sigma(I)$]	R1 = 0.0270, wR2 = 0.0733
R indices (all data)	R1 = 0.0342, wR2 = 0.0779
extinction coeff	0.00000(7)
largest diff peak and hole	0.967 and −0.897 e Å^{-3}

Table 2. Bond Lengths [Å] and Angles [deg] for $[Ar_{Cl}N_2NMe]Hf(i\text{-}Bu)_2$

Hf−N(1)	2.104(3)	N(3)−Hf−C(1)	139.59(12)
Hf−N(2)	2.105(3)	N(3)−Hf−C(5)	118.79(11)
Hf−N(3)	2.378(3)	C(1)−Hf−C(5)	101.62(14)
Hf−C(1)	2.220(4)	C(20)−N(2)−Hf	124.39(19)
Hf−C(5)	2.207(3)	C(11)−N(2)−Hf	123.7(2)
N(1)−Hf−N(2)	141.77(10)	C(14)−N(1)−Hf	123.1(2)
N(1)−Hf−C(1)	100.48(11)	C(9)−N(1)−Hf	124.4(2)
N(1)−Hf−C(5)	103.17(12)	C(6)−C(5)−Hf	126.6(2)
N(1)−Hf−N(3)	71.19(10)	C(12)−N(3)−Hf	106.2(2)
N(2)−Hf−C(1)	102.49(11)	C(10)−N(3)−Hf	107.0(2)
N(2)−Hf−C(5)	101.61(12)	C(13)−N(3)−Hf	111.5(2)
N(2)−Hf−N(3)	71.47(10)	C(2)−C(1)−Hf	123.8(3)

pounds of this type. The Hf−N_{amido} and Hf−C_α bond distances are within the expected range. The $CHMe_2$ group of the syn isobutyl group is turned away from the NMe group toward the anti isobutyl group, pushing the $CHMe_2$ group of the anti isobutyl group away. The Hf−C_α−C_β angles are similar (123.8° and 126.6°). There is no significant interaction between the metal and one of the ortho chlorides in the aryl group, which was found to be the case in a related complex, $[(2,6\text{-}Cl_2C_6H_3NHCH_2)_2C(CH_3)(2\text{-}C_5H_4N)]Hf(i\text{-}Bu)_2$.[29]

Addition of 1 or more equiv of i-BuMgCl to $[Ar_{Cl}N_2NMe]HfCl_2$ led to formation of $[Ar_{Cl}N_2NMe]$-Hf(i-Bu)Cl. Samples of $[Ar_{Cl}N_2NMe]Hf(i\text{-}Bu)Cl$ were found to consist of two isomers, presumably those in which either the alkyl or the chloride is in the "syn" position nearest the NMe group. Recrystallization of mixtures of isomers of $[Ar_{Cl}N_2NMe]Hf(i\text{-}Bu)Cl$ from ether resulted in a mixture that contained ∼75% $[Ar_{Cl}N_2NMe]Hf(i\text{-}Bu_{syn})Cl_{anti}$, according to the chemical shift of the isobutyl methylene group.

The reaction of $[Ar_{Cl}N_2NMe]Hf(i\text{-}Bu)Cl$ with 1 equiv of MeMgCl afforded $[Ar_{Cl}N_2NMe]Hf(i\text{-}Bu)Me$. Samples enriched in $[Ar_{Cl}N_2NMe]Hf(i\text{-}Bu_{anti})Cl_{syn}$ or $[Ar_{Cl}N_2NMe]$-$Hf(i\text{-}Bu_{syn})Cl_{anti}$ form $[Ar_{Cl}N_2NMe]Hf(i\text{-}Bu)Me$ mixtures that are enriched in the analogous isomer, according to ^{1}H NOESY experiments. Mixtures of $[Ar_{Cl}N_2NMe]$-$Hf(i\text{-}Bu_{syn})Me_{anti}$ and $[Ar_{Cl}N_2NMe]Hf(i\text{-}Bu_{anti})Me_{syn}$ then evolve to yield an equilibrium mixture of the two, with the isomer in which the methyl group is in the "syn" position predominating at higher temperatures. The anti/syn isomerization process for $[Ar_{Cl}N_2NMe]Hf(i\text{-}Bu)$-Me between 30 and 90 °C was found to follow first-order kinetics. At temperatures higher than 70 °C, slow β-hydride elimination occurs and isobutene gradually appears in the ^{1}H NMR spectrum. During the isomerization of $[Ar_{Cl}N_2NMe]Hf(i\text{-}Bu_{syn})Me_{anti}$ to $[Ar_{Cl}N_2NMe]$-$Hf(i\text{-}Bu_{anti})Me_{syn}$, which we call $Me_{anti} \rightarrow Me_{syn}$ isomerization, neither $[Ar_{Cl}N_2NMe]Hf(i\text{-}Bu)_2$ nor $[Ar_{Cl}N_2NMe]$-$HfMe_2$ is observed. The rate constants measured for the $Me_{anti} \rightarrow Me_{syn}$ process at different temperatures using a first-order approach to equilibrium are listed in the Experimental Section. The $Me_{anti} \rightarrow Me_{syn}$ conversion was found to take place with $\Delta H^\ddagger = 82.9$ kJ/mol and $\Delta S^\ddagger = -65.7$ J/molK and with $\Delta H = 2.2$ kJ/mol and $\Delta S = 8.3$ J/mol K. We do not know whether the ligand's central nitrogen donor remains bound to the metal or not during the $Me_{anti} \rightarrow Me_{syn}$ conversion process, and the $\Delta S^\ddagger$ value is not especially helpful in answering this question.

Activation of Dialkyl Complexes. Addition of 1 equiv of $\{Ph_3C\}\{B(C_6F_5)_4\}$ to $[Ar_{Cl}N_2NMe]MMe_2$ (M = Hf, Zr) in bromobenzene-d_5 at −30 °C produced $\{[Ar_{Cl}N_2NMe]MMe\}\{B(C_6F_5)_4\}$ and Ph_3CCH_3 quantitatively and was accompanied by an immediate color change of the solution from deep orange to yellow. Proton NMR spectra of the zirconium and hafnium cations at 0 °C are almost identical. The backbone methylene protons appear as four well-resolved multiplets between 2.6 and 3.9 ppm, and the NMe resonance appears at 2.3 ppm for both hafnium and zirconium complexes. Free rotation of the aryl rings is evidenced by the presence of a sharp doublet representing four equivalent meta protons. Sharp MMe resonances are found at 0.49 ppm for hafnium and 0.62 ppm for zirconium. While the zirconium and hafnium methyl cations are stable at 0 °C for at least 24 h, both species slowly decompose at roughly similar rates at temperatures greater than 40 °C. Multiple decomposition products appeared to form, and none could be identified.

Scheme 2. Insertion of Isobutene into {[$Ar_{Cl}N_2$NMe]Hf(i-Bu)}{$B(C_6F_5)_4$}

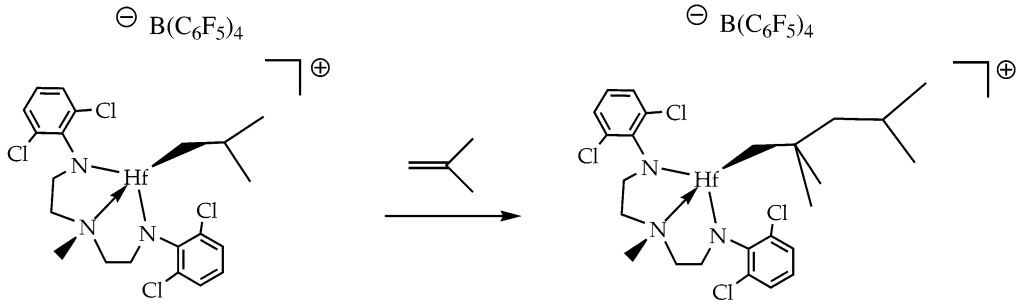

Abstraction of a methyl group from [$Ar_{Cl}N_2$NMe]-MMe_2 (M = Hf, Zr) by $B(C_6F_5)_3$ in C_6D_5Br at −30 °C yielded {[$Ar_{Cl}N_2$NMe]MMe}{$MeB(C_6F_5)_3$}. The reaction solution acquired a yellow color a few seconds after addition of $B(C_6F_5)_3$ as the cationic complex was formed. Proton NMR spectra of hafnium and zirconium methyl cations paired with the $\{MeB(C_6F_5)_3\}^-$ anion are essentially identical to those paired with the $\{B(C_6F_5)_4\}^-$ anion. These complexes are also stable at 0 °C for at least 24 h, and there is no significant difference in the stability of zirconium versus hafnium methyl cations.

As communicated previously,[28] protonation of a Zr−Me group in [$Ar_{Cl}N_2$NMe]$ZrMe_2$ with {$PhNMe_2H$}-{$B(C_6F_5)_4$} in bromobenzene at −20 °C produced methane and {[$Ar_{Cl}N_2$NMe]ZrMe($PhNMe_2$)}{$B(C_6F_5)_4$}, which has mirror symmetry on the NMR time scale. The analogous activation of [$Ar_{Cl}N_2$NMe]$HfMe_2$ with {$PhNMe_2H$}{$B(C_6F_5)_4$} yielded {[$Ar_{Cl}N_2$NMe]HfMe-($PhNMe_2$)}{$B(C_6F_5)_4$}, which also has mirror symmetry. As the temperature is lowered from room temperature to −10 °C, the Hf−Me resonance at 0.2 ppm broadens considerably compared to the Zr−Me resonance. We propose that this reversible process involves unsymmetrical interaction of bromobenzene with the metal center or hindered rotation of bound dimethylaniline about the M−N bond, or both. Free dimethylaniline is observed in the ^{1}H NMR spectra of both hafnium and zirconium cations at temperatures higher than 40 °C.

Addition of $B(C_6F_5)_3$ to [$Ar_{Cl}N_2$NMe]Hf(i-$Bu)_2$ almost immediately yielded isobutene and pale yellow {[$Ar_{Cl}N_2$NMe]Hf(i-Bu)}{$HB(C_6F_5)_3$}. In bromobenzene-d_5 at 0 °C, the isobutyl CH_3 and CH_2 resonances appear as broadened singlets at 0.91 and 0.96 ppm, respectively. On the basis of integration values, the methine resonance appears to overlap with the ligand NMe resonance at 2.58 ppm and cannot be distinguished from the NMe resonance as the temperature is varied from −30 to 40 °C. Resonances outside the range of 0−10 ppm are not observed. Broadening of the isobutyl resonances can be attributed to exchange processes that involve anion or solvent binding to the metal in various ways. In toluene, the expected splitting pattern for a freely rotating isobutyl group is observed (isobutyl CH_3 and CH_2 resonances are doublets found at 0.88 and 1.02 ppm, respectively). The methine resonance again appears to overlap with the NMe resonance as well as with a ligand ethylene resonance at 2.39 ppm.

Activation of [$Ar_{Cl}N_2$NMe]Hf(i-$Bu)_2$ with {Ph_3C}-{$B(C_6F_5)_4$} in bromobenzene-d_5 at 0 °C yielded isobutene, {[$Ar_{Cl}N_2$NMe]Hf(i-Bu)}{$B(C_6F_5)_4$}, and Ph_3CH and was accompanied by an immediate color change of the solution from deep orange to yellow. The isobutyl CH_3 and CH_2 ^{1}H NMR resonances of the {[$Ar_{Cl}N_2$NMe]-Hf(i-Bu)}$^+$ ion also appear as broadened singlets at 0 °C, and the ^{1}H NMR spectrum is not markedly different from that of {[$Ar_{Cl}N_2$NMe]Hf(i-Bu)}{$HB(C_6F_5)_3$}. Chemical shifts for the four ligand ethylene CH_2 resonances and the two ligand aryl proton resonances for these isobutyl cations are nearly identical to the corresponding shifts in the hafnium methyl cations.

The hafnium isobutyl cation, paired with either the $\{HB(C_6F_5)_3\}^-$ or $\{B(C_6F_5)_4\}^-$ anion, slowly reacts with isobutene produced during activation to afford what is proposed, on the basis of NMR data, to be the 1,2 insertion product of isobutene into the M−R bond of the isobutyl cation (Scheme 2). A downfield shift of the NMe resonance from 2.58 to 2.60 ppm is observed for the cation with the longer alkyl chain. The insertion product began to decompose after several hours at 0 °C; complete insertion required 1.5 weeks at −30 °C. Therefore it was not possible to generate a pure sample of the insertion product. Addition of 1-hexene to a solution that contained the insertion product at 0 °C resulted in consumption of the insertion product and polymerization behavior that was not significantly different from that of the isobutyl cation. Under 1 atm of isobutene gas at 0 °C, {[$Ar_{Cl}N_2$NMe]Hf(i-Bu)}{$HB(C_6F_5)_3$} (formed by the activation of [$Ar_{Cl}N_2$NMe]Hf(i-$Bu)_2$ with $B(C_6F_5)_3$) oligomerized isobutene.

Protonation of [$Ar_{Cl}N_2$NMe]Hf(i-$Bu)_2$ with 1 equiv of {$PhNMe_2H$}{$B(C_6F_5)_4$} in bromobenzene produced isobutane, {[$Ar_{Cl}N_2$NMe]Hf(i-Bu)}{$B(C_6F_5)_4$}, and free dimethylaniline. {[$Ar_{Cl}N_2$NMe]Hf(i-Bu)}{$B(C_6F_5)_4$} then slowly reacted with the dimethylaniline to form isobutene and an asymmetric complex that is not active for polymerization of 1-hexene. The asymmetric decomposition product also was observed upon addition of dimethylaniline to {[$Ar_{Cl}N_2$NMe]Hf(i-Bu)}{$HB(C_6F_5)_3$} (formed by activation of [$Ar_{Cl}N_2$NMe]Hf(i-$Bu)_2$ with $B(C_6F_5)_3$). Complete conversion of the isobutyl cation to the asymmetric decomposition product was not observed even when 10 equiv of dimethylaniline was added and the solution stored at −30 °C for several weeks. According to ^{1}H NMR studies, added diethyl ether coordinates to the isobutyl cation, but not to the asymmetric decomposition product. Unfortunately, this asymmetric decomposition product could not be identified using 1D and 2D (gCOSY) NMR techniques. Note that we have seen a reaction between dimethylaniline and {[$(MesNCH_2)_2C(CH_3)(2\text{-}C_5H_4N)$]Hf(i-Bu)}$^+$ that yields isobutane and a species with mirror symmetry that is proposed to contain an *o*-dimethylaminophenyl group.[30] The asymmetric decomposition product found here cannot be the same type as the one that contains the

Table 3. Poly[1-hexene] Prepared Using the {[$Ar_{Cl}N_2$NMe]ZrMe}{$B(C_6F_5)_4$} Initiator

T (°C)	solvent	[Zr] (M)	equiv	M_n (f/calc)[a]	PDI	$\beta_{1,2}$-H[b]	k_p ($M^{-1}s^{-1}$)
0	C_6H_5Cl	0.003	100	1.12	1.07		
0	C_6H_5Cl	0.003	200	0.97	1.10		
0	C_6H_5Cl	0.003	300	0.95	1.10		
0	C_6H_5Cl	0.003	400	0.97	1.08		
0	C_6H_5Cl	0.003	500	0.96	1.08		
0	C_6D_5Br	0.003	300			0.1	0.63
0	C_6D_5Br	0.006	100			0.1	0.85
−30	C_6H_5Br	0.006	200	1.1	1.08		

[a] M_n(found)/M_n(calcd). [b] $\beta_{1,2}$-H = β-hydride elimination following a 1,2 insertion versus initiator.

o-dimethylaminophenyl group, but we believe it might result from a related CH activation process.

It would be possible to study the polymerization behavior of the hafnium isobutyl complex in the absence of isobutene if a methyl group could be abstracted from [$Ar_{Cl}N_2$NMe]Hf(i-Bu)Me selectively. The reaction between mixtures of [$Ar_{Cl}N_2$NMe]Hf(i-Bu)Me isomers and {Ph_3C}{$B(C_6F_5)_4$} in bromobenzene-d_5 at 0 °C yielded 72% {[$Ar_{Cl}N_2$NMe]Hf(i-Bu)}{$B(C_6F_5)_4$} and 28% {[$Ar_{Cl}N_2$NMe]Hf(Me)}{$B(C_6F_5)_4$}. Activation of [$Ar_{Cl}N_2$NMe]Hf(i-Bu)Me isomers with $B(C_6F_5)_3$ led to the nearly selective abstraction of a methyl group and the formation of about 95% {[$Ar_{Cl}N_2$NMe]Hf(i-Bu)}{$MeB(C_6F_5)_3$}. Protonolysis by {$PhNMe_2H$}{$B(C_6F_5)_4$} resulted in formation of {[$Ar_{Cl}N_2$NMe]Hf(i-Bu)}{$B(C_6F_5)_4$} exclusively, which subsequently reacted with dimethylaniline as described above. The outcome of activation of the mixed dialkyl species does not appear to depend to a significant degree on which isomer of the mixed alkyl complex predominates in the mixture. On the basis of these results, 100% selective removal of a methyl group in the isobutyl/methyl species does not appear to be possible under the conditions we have employed so far.

Polymerization of 1-Hexene. Consumption of up to 500 equiv of 1-hexene by the {[$Ar_{Cl}N_2$NMe]MMe}$^+$ (M = Hf, Zr) initiator, formed by activation of [$Ar_{Cl}N_2$NMe]MMe_2 with either {Ph_3C}{$B(C_6F_5)_4$} or $B(C_6F_5)_3$, is rapid and nearly complete within minutes at 0 °C and therefore difficult to follow using ordinary NMR techniques. At zirconium catalyst concentrations up to 6 mM, plots of ln[1-hexene] versus time for the final 4−8% of the polymerization were linear, with k_p values ranging between 0.63 and 0.85 M^{-1} s^{-1} (Table 3). These values agree with the value of 0.80 M^{-1} s^{-1} estimated for polymerization of 1-hexene by {[$Ar_{Cl}N_2$NMe]ZrMe}{$B(C_6F_5)_4$} in the absence of dimethylaniline base.[28] The consumption of the final 13% of 1-hexene at 0 °C by {[$Ar_{Cl}N_2$NMe]HfMe}{$B(C_6F_5)_4$} (Figure 2) revealed lower k_p values between 0.15 and 0.25 M^{-1} s^{-1} (Table 4). In all reactions, {[$Ar_{Cl}N_2$NMe]MMe}{$B(C_6F_5)_4$} was completely consumed in the presence of 100 or more equiv of 1-hexene.

Polymerization of 100−500 equiv of 1-hexene by 3 mM {[$Ar_{Cl}N_2$NMe]ZrMe}{$B(C_6F_5)_4$} in chlorobenzene at 0 °C yielded poly[1-hexene] with M_n values close to those calculated for a perfectly living system (Figure 3, Table 3) and with PDI values ranging from 1.07 to 1.10. While the product of β-hydride elimination following a 2,1 insertion of 1-hexene ("$\beta_{2,1}$ product") was not observed, a broad vinylidene resonance corresponding to the olefinic product of β-hydride elimination following a 1,2 insertion ("$\beta_{1,2}$ product") grew in at 4.86 ppm in the ^{1}H NMR spectrum as 1-hexene was consumed. The final amount of the $\beta_{1,2}$ product was approximately 10% of the initiator present.

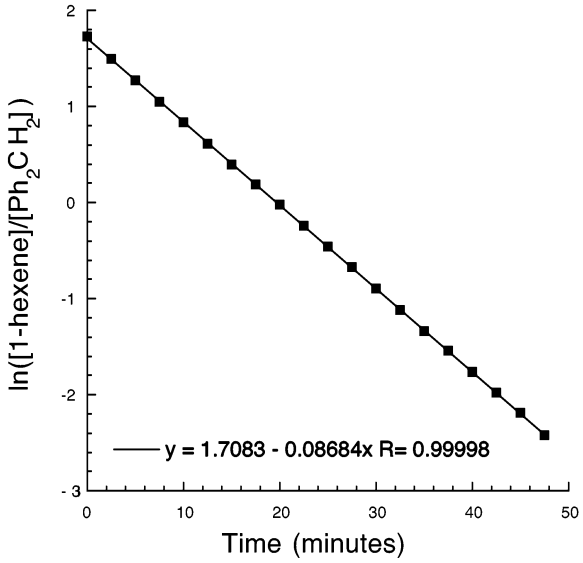

Figure 2. Consumption of the final 13% of 100 equiv of 1-hexene at 0 °C by 0.006 M {[$Ar_{Cl}N_2$NMe]HfMe}{$B(C_6F_5)_4$} (formed by the activation of [$Ar_{Cl}N_2$NMe]$HfMe_2$ with {Ph_3C}{$B(C_6F_5)_4$}).

When {[$Ar_{Cl}N_2$NMe]HfMe}{$B(C_6F_5)_4$} or {[$Ar_{Cl}N_2$NMe]HfMe}{$MeB(C_6F_5)_3$} was employed as an initiator at 0 °C, the resulting poly[1-hexene] had PDI values that ranged from 1.1 to 1.4 (Table 4). These systems are susceptible to a significant amount of 1,2 β-hydride elimination and slower rates of initiation than propagation. Olefinic resonances between 5.3 and 5.5 ppm ascribed to a $\beta_{2,1}$ product were observed in amounts up to 0.5 equiv of the initiator present. An olefinic resonance for the $\beta_{1,2}$ product grew in at 4.86 ppm in the ^{1}H NMR spectrum as 1-hexene was consumed (to between 0.6 and 1.5 equiv versus initiator) and continued to grow to approximately 1 equiv versus initiator after all 1-hexene had been consumed. GPC analysis revealed a multimodal trace, with $M_{n(found)}/M_{n(calcd)}$ ratios for the primary peaks (in bold) ranging from 0.4 to 0.9 for the polymerization of 100−400 equiv of 1-hexene at 0 °C (Table 4). While premature termination reactions were limited at −30 °C, low molecular weight peaks with $M_{n(found)}/M_{n(calcd)}$ ratios of about 0.2 were observed for polymerizations at 0 °C. Lower than expected experimental M_n values, as well as pseudo-first-order kinetics for consumption of 1-hexene, suggest that the hafnium product of β-hydride elimination is still active for polymerization.

Polymer analysis of reactions employing the {[$Ar_{Cl}N_2$NMe]HfMe}$^+$ initiator at −30 °C also showed significant high molecular weight peaks with $M_{n(found)}/M_{n(calcd)}$ ratios of 24.8 and 6.2, resulting from a greater rate of propagation than initiation. To eliminate initiation problems observed when the hafnium methyl

(30) Mehrkhodavandi, P.; Pryor, L. L.; Schrock, R. R. *Organometallics* **2003**, *22*, 4569.

Table 4. Poly[1-hexene] Prepared Using the {[$Ar_{Cl}N_2$NMe]HfMe}$^+$ Initiator

T (°C)	[Hf] (M)	anion	equiv	peak ratio[a]	PDI	M_n (f/c)[b]	$\beta_{1,2}$-H[c]	k_p (M^{-1} s^{-1})
−30	0.006	{$B(C_6F_5)_4$}$^-$	200	1	1.23	24.8		
				5	1.07	6.2		
				19	**1.04**	**1.1**		
0	0.006	{$B(C_6F_5)_4$}$^-$	100	1	1.10	4.0	0.6	0.24
				7	**1.10**	**0.8**		
0	0.012	{$B(C_6F_5)_4$}$^-$	100	1	1.06	4.3	0.9	0.25
				10	**1.26**	**0.7**		
				2	1.30	0.2		
0	0.012	{$B(C_6F_5)_4$}$^-$	269	1	1.05	4.1		
				6	**1.30**	**0.8**		
				1	1.69	0.4		
0	0.003	{$B(C_6F_5)_4$}$^-$	400	1	1.08	5.2	0.6	0.15
				4	**1.36**	**0.7**		
0	0.006	{$B(C_6F_5)_4$}$^-$	400	1	1.09	3.2	1.5	0.17
				6	**1.43**	**0.4**		
0	0.006	{$MeB(C_6F_5)_3$}$^-$	200	1	1.08	4.6	0.4	0.19
				7	**1.19**	**0.9**		

[a] Relative areas of peaks in BPC trace (refractive index detector). [b] M_n(found)/M_n(calcd). [c] $\beta_{1,2}$-H = β-hydride elimination following a 1,2 insertion versus initiator.

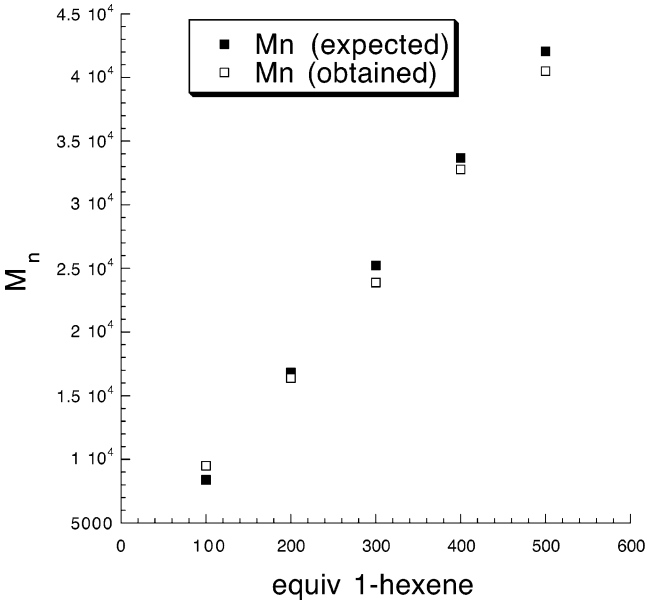

Figure 3. Molecular weights of poly[1-hexene] obtained with 3 mM {[$Ar_{Cl}N_2$NMe]ZrMe}{$B(C_6F_5)_4$} as the initiator in chlorobenzene at 0 °C.

cations were employed, [$Ar_{Cl}N_2$NMe]Hf(i-Bu)$_2$ was employed as a precatalyst, since the greater steric bulk of the isobutyl group is sterically more like the alkyl in the growing polymer chain. If 1-hexene is added immediately after [$Ar_{Cl}N_2$NMe]Hf(i-Bu)$_2$ and the activator are mixed, the insertion of 1-hexene should be greatly preferred over the relatively slow insertion of isobutene.

The rate of polymerization by {[$Ar_{Cl}N_2$NMe]Hf(i-Bu)}{$B(C_6F_5)_4$} was not significantly different than the rate of polymerization by {[$Ar_{Cl}N_2$NMe]HfMe}{$B(C_6F_5)_4$}. PDI values of the resulting poly[1-hexene] ranged from 1.1 to 1.3, and experimental M_n values were approximately half of those calculated for a perfectly living system (Table 5). GPC analysis of the polymer formed at −30 °C revealed a single sharp peak with a large sloping low molecular weight tail (refractive index detector). No high molecular weight peak was observed. The overall PDI was 1.16 and the $M_{n(found)}/M_{n(calcd)}$ ratio was 0.88. The polymerization of 1-hexene at 0 and −30 °C by {[$Ar_{Cl}N_2$NMe]Hf(i-Bu)}{$MeB(C_6F_5)_3$}, formed by the activation of [$Ar_{Cl}N_2$NMe]Hf(i-Bu)Me with $B(C_6F_5)_3$,

Table 5. Poly[1-hexene] Prepared Using the {[$Ar_{Cl}N_2$NMe]Hf(i-Bu)}$^+$ Initiator

T (°C)	[Hf] (M)	anion	equiv	PDI	M_n (f/c)[a]	$\beta_{1,2}$-H[b]	k_p (M^{-1} s^{-1})
−30	0.006	{$B(C_6F_5)_4$}$^-$	200	1.16	0.88		
0	0.003	{$B(C_6F_5)_4$}$^-$	500	1.28	0.55		
0	0.003	{$B(C_6F_5)_4$}$^-$	300	1.25	0.59	1.4	0.13
0	0.013	{$HB(C_6F_5)_3$}$^-$	50			1.0	0.25
0	0.012	{$B(C_6F_5)_4$}$^-$	100	1.20	0.51	1.9	

[a] M_n(found)/M_n(calcd). [b] $\beta_{1,2}$-H = β-hydride elimination following a 1,2 insertion versus initiator.

proceeded at a rate essentially identical to that of the isobutyl cation in the presence of isobutene to produce poly(1-hexene) having similar PDI values and $M_{n(found)}/M_{n(calcd)}$ ratios.

During polymerization of 1-hexene by hafnium methyl or isobutyl cations, the initiator was completely consumed and the active propagating species was generated. The propagating species is characterized by a new set of broadened ligand resonances in the ^{1}H NMR spectrum. After consumption of 1-hexene was complete, these broadened resonances were gradually replaced by sharp ligand resonances characteristic of a single (nonpolymeric) cationic species. There appears to be a direct relationship between the growth of this hafnium product and the olefinic $\beta_{1,2}$ product resonance at 4.86 ppm. Upon complete consumption of 1-hexene by {[$Ar_{Cl}N_2$NMe]Hf(i-Bu)}{$HB(C_6F_5)_3$} at 0 °C, the growth of the olefinic resonance at 4.86 ppm and a ligand ethylene CH_2 resonance at 3.9 ppm were each measured in comparison to an internal standard. The concentrations of these species in relation to the concentration of the initiator (calculated from the integration of [Ph_2CH_2]) were plotted as a function of time (Figure 4). Any isobutene remaining in solution did not appear to be involved in the process, and the use of the $B(C_6F_5)_3$ activator ensured that the olefinic β-hydride elimination product would not be polymerized by trace amounts of Ph_3C^+.

To determine whether the hafnium product of β-hydride elimination was still active for the polymerization, 1-hexene was added in two batches consecutively. Polymerization of 300 equiv of 1-hexene by {[$Ar_{Cl}N_2$NMe]Hf(i-Bu)}{$B(C_6F_5)_4$} at 0 °C resulted in a k_p of 0.13 M^{-1} s^{-1} and an $M_{n(found)}/M_{n(calcd)}$ ratio of 0.6.

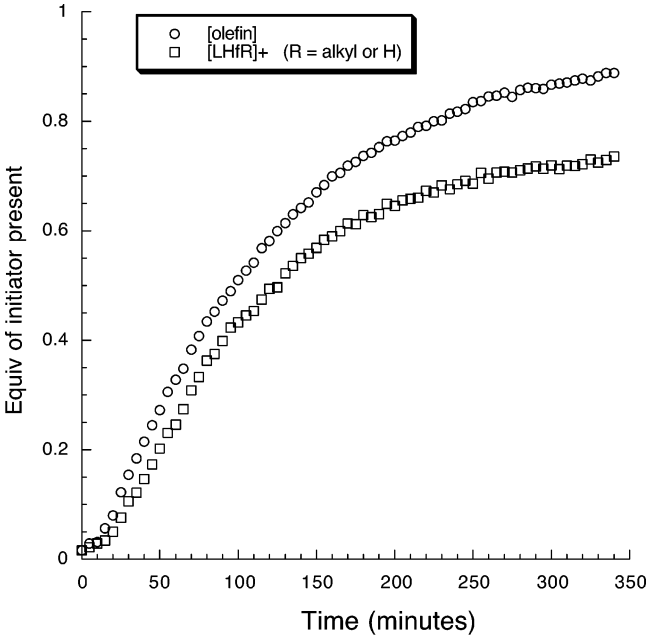

Figure 4. Growth of hafnium complex and olefin upon decomposition of propagating species after completion of 1-hexene polymerization by $\{[Ar_{Cl}N_2NMe]Hf(i\text{-}Bu)\}\{HB(C_6F_5)_3\}$ at 0 °C in bromobenzene-d_5.

Table 6. Equivalents of β-Hydride Elimination versus Initiator Present after Polymerization of Two Successive 300 Equiv of 1-Hexene by $\{[Ar_{Cl}N_2NMe]Hf(R)\}\{B(C_6F_5)_4\}$

	$\beta_{2,1}$-H product	$\beta_{1,2}$-H product	$\beta_{1,2}$-H product (16 h)
first 300 equiv	1.0 equiv	1.4 equiv	2.3 equiv
second 300 equiv	3.0 equiv	3.7 equiv	4.7 equiv

After 10 h, a ^{1}H NMR spectrum showed that the propagating species had decomposed by β-hydride elimination, and another 300 equiv of 1-hexene was added to the solution at 0 °C. The resonances for the propagating chain reappeared in the ^{1}H NMR spectrum, and 1-hexene was polymerized with an identical k_p of 0.13 M^{-1} s^{-1} and the overall $M_{n(found)}/M_{n(calcd)}$ ratio was found to be 0.3. Six hours after the second batch of 1-hexene was consumed, the resonances for the hafnium product of β-hydride elimination reemerged. Another 1.0 equiv of olefin product was produced during this postpolymerization period to give a total of 4.7 equiv of 1,2 β-hydride elimination and 3.0 equiv of 2,1 β-hydride elimination (Table 6). The low molecular weight of the polymer and the observed pseudo-first-order kinetics despite extensive β-hydride elimination suggest that the hafnium product of β-hydride elimination is indeed active for the polymerization of 1-hexene. Unfortunately, we have not been able to identify the product of β-hydride elimination.

Conclusions

Replacement of the mesityl substituents in $[(MesitylNCH_2CH_2)_2NMe]^{2-}$ with 2,6-$Cl_2C_6H_3$ groups prevented rampant decomposition of the propagating species through CH activation. Living characteristics were observed for zirconium catalysts. On the basis of polydispersities and the molecular weights of the poly-[1-hexene] that is formed, the behavior of these catalysts is similar to that of the recently reported $[(2,6\text{-}Cl_2C_6H_3NCH_2)_2C(CH_3)(2\text{-}C_5H_4N)]^{2-}$ hafnium catalysts.[29]

In contrast to the zirconium catalysts, hafnium catalysts that contain the $[(2,6\text{-}C_6H_3Cl_2NCH_2CH_2)_2NMe]^{2-}$ ligand are prone to significant 1,2 and 2,1 β-hydride elimination. On the basis of the quantity of β-hydride elimination when polymer yields are 100%, the hafnium product of β-hydride elimination appears to initiate the polymerization of 1-hexene at a rate equal to that of the methyl or isobutyl initiator. Therefore the hafnium product of β-hydride elimination appears to be relatively stable under the reaction conditions.

The presence of chlorides in the 2 and 6 positions of aryl substituents instead of methyl groups has been shown to lead to a decrease in catalytic activity for the $\{[(2,6\text{-}Cl_2C_6H_3NCH_2)_2C(CH_3)(2\text{-}C_5H_4N)]HfR\}\{B(C_6F_5)_4\}$ catalyst ($k_p \approx 0.05$ M^{-1} s^{-1} for 1-hexene at 0 °C) compared to the $\{[(MesitylNCH_2)_2C(CH_3)(2\text{-}C_5H_4N)]HfR\}\{B(C_6F_5)_4\}$ catalyst ($k_p \approx 0.10$ M^{-1} s^{-1}).[29,30] A similar comparison between the $\{[(2,6\text{-}Cl_2C_6H_3NCH_2CH_2)_2NMe]ZrR\}\{B(C_6F_5)_4\}$ catalyst ($k_p \approx 0.80$ M^{-1} s^{-1}) and the $\{[(MesitylNCH_2CH_2)_2NMe]Zr(PhNMe_2)R\}\{B(C_6F_5)_4\}$ catalyst (estimated $k_p \approx 4.8$ M^{-1} s^{-1}) may be compromised by the assumptions involved in obtaining the 4.8 M^{-1} s^{-1} value.[13] Both the hafnium and zirconium $\{[(2,6\text{-}Cl_2C_6H_3NCH_2CH_2)_2NMe]MR\}\{B(C_6F_5)_4\}$ catalysts display higher activity than the $\{[(ArNCH_2)_2C(CH_3)(2\text{-}C_5H_4N)]HfR\}\{B(C_6F_5)_4\}$ (Ar = mesityl or 2,6-$Cl_2C_6H_3$) catalysts. The hafnium catalyst $\{[(2,6\text{-}Cl_2C_6H_3NCH_2CH_2)_2NMe]HfR\}\{B(C_6F_5)_4\}$ ($k_p \approx 0.20$ M^{-1} s^{-1}) is slower than the analogous zirconium catalyst ($k_p \approx 0.80$ M^{-1} s^{-1}). In comparison, the rates of polymerization by hafnium and zirconium catalysts of the type $\{[(MesitylNCH_2)_2C(CH_3)(2\text{-}C_5H_4N)]MR\}\{B(C_6F_5)_4\}$ are essentially identical with $k_p \approx 0.10$ M^{-1} s^{-1}.[29,30]

Experimental Section

General Details. All reactions were performed under an atmosphere of dinitrogen in a Vacuum Atmospheres drybox or using Schlenk techniques, and catalyst activation was performed in a drybox free of ether, THF, and other coordinating solvents. Nondeuterated solvents were sparged with nitrogen for 45 min followed by passage through a 1 gallon column of activated alumina.[31] Bromobenzene, chlorobenzene, and deuterated solvents were stirred over CaH_2 for 48 h, vacuum-transferred, and stored over 4 Å molecular sieves. $Hf(NMe_2)_4$ and $Zr(NMe_2)_4$ were synthesized according to reported methods.[32] Unlabeled Grignard reagents were purchased from Aldrich and titrated prior to use with 4-cumylphenol or 1-propanol using 1,10-phenanthrolene as an indicator. All other commercial reagents were used without further purification. NMR data were recorded using Varian Inova-500, Bruker AVANCE-400, Varian Unity-300, or Varian Mercury-300 spectrometers. Chemical shifts are reported in parts per million (ppm). The residual protons or ^{13}C atoms of the deuterated solvents were used as internal references. Elemental analyses (C, H, N, Cl) were done by Kolbe Mikroanalytisches Laboratorium, Mülheim an der Ruhr, Germany. GPC analyses were conducted using a system equipped with two Waters 7.8 × 300 mm columns (Ultrastyragel 10^4 Å and Styragel HR5E) in series and a Wyatt Technology mini Dawn light scattering detector coupled with a Knauer differential

(31) Pangborn, A. B.; Giardello, M. A.; Grubbs, R. H.; Rosen, R. K.; Timmers, F. J. *Organometallics* **1996**, *15*, 1518.
(32) Diamond, G. M.; Jordan, R. F.; Petersen, J. L. *Organometallics* **1996**, *15*, 4030.

refractometer. A Knauer 64 HPLC pump was used to supply HPLC grade THF at a flow rate of 1.0 mL/min. The auxiliary constant of the apparatus (5.9×10^{-4}) was calibrated using a polystyrene standard ($M_n = 2.2 \times 10^5$), and M_n and M_w values for poly(1-hexene) were obtained using $dn/dc = 0.076$ mL/gr (Wyatt Technology). Data analysis was carried out using Astrette 1.2 software (Wyatt Technology).

(2,6-$C_6H_3Cl_2NHCH_2CH_2)_2NH$ ($H_2[Ar_{Cl}N_2NH]$). BINAP (0.664 g, 1.07 mmol) was taken up in toluene (100 mL), and the resulting suspension was heated until the BINAP dissolved. $Pd(dba)_3$ (0.488 g, 0.533 mmol) was added, and the gray solution was heated until the reaction acquired an orange tint. The solution was filtered through packed Celite, combined with $HN(CH_2CH_2NH_2)_2$ (3.668 g, 35.6 mmol), 2-bromo-1,3-dichlorobenzene (16.06 g, 71.11 mmol), and NaOt-Bu (10.59 g, 110.2 mmol) in toluene (250 mL), transferred to a sealed Schlenk flask, and heated at 95 °C for 17 h under N_2. The hot reaction mixture was filtered through alumina, and toluene was removed in vacuo. The product was extracted in Et_2O (120 mL) against H_2O (2×80 mL) and saturated NaCl solution (80 mL) and combined with Et_2O (2×40 mL) containing product recovered through back-extraction with H_2O portions. The Et_2O portions were concentrated in vacuo to yield an impure brown oil, which was dissolved in toluene and filtered through a silica gel plug column. Toluene (750 mL) was passed through 200 mL of silica gel to wash out impurities, and the product was flushed out with Et_2O. After the solvent was removed, the resulting orange powder was recrystallized from Et_2O (50 mL) at 0 °C to afford transparent crystals; yield 7.759 g (56%). ^1H NMR (C_6D_6): δ 0.48 (br s, 1H, NH), 2.36 and 3.23 (m, 4H each, ligand CH_2), 4.76 (br t, 2H, ArylNH), 6.24 (t, 2H, p-H), 6.96 (d, 4H, m-H). FAB-MS: positive ion $(M + H)^+$, measured (calcd) 392.0242 ± 0.0012 (392.0255).

(2,6-$C_6H_3Cl_2NHCH_2CH_2)_2NMe$ ($H_2[Ar_{Cl}N_2NMe]$). K_2CO_3 (3.23 g, 23.4 mmol) was added to a solution of $H_2[Ar_{Cl}N_2NH]$ (2.52 g, 6.41 mmol) in 125 mL of anhydrous CH_3CN. The reaction was sparged with N_2 for 15 min, and MeI (0.459 mL, 6.73 mmol) was added dropwise via syringe with vigorous stirring. The reaction was stirred for 24 h, and a white suspension was filtered off. All volatile components were removed, and the residue was worked up with a mixture of ether and water. The organic layer was separated, washed several times with water, and dried over $MgSO_4$. Removal of solvent in vacuo gave a pale yellow powder; yield 1.66 g (63%). ^1H NMR ($CDCl_3$): δ 2.31 (s, 3H, NCH_3), 2.66 and 3.45 (m, 4H each, ligand CH_2), 4.76 (br s, 2H, ArylNH), 6.76 (t, 2H, p-H), 7.23 (d, 4H, m-H). FAB-MS: positive ion $(M + H)^+$, measured (calcd): 406.0421 ± 0.0012 (406.0411).

$[Ar_{Cl}N_2NMe]Zr(NMe_2)_2$. $Zr(NMe_2)_4$ (1.091 g, 4.078 mmol) was added to a solution of $H_2[Ar_{Cl}N_2NMe]$ (1.660 g, 4.077 mmol) in benzene (10 mL). The reaction was stirred for 16 h at room temperature. As the reaction was concentrated in vacuo, a white solid precipitated. The product was collected via filtration and washed with pentane to give a white powder; yield 1.979 g (83%). ^1H NMR ($C_6D_5CD_3$): δ 2.31 (s, 3, NCH_3), 3.31 and 2.55 (s, 6H each, NMe_2), 3.05, 3.25, 3.92 (m, 8H, ligand CH_2), 6.42 (t, 2H, p-H), 7.12 (d, 4H, m-H). Anal. Calcd for $ZrCl_4N_5C_{21}H_{29}$: C, 43.15; H, 5.00; N, 11.98; Cl, 24.26. Found: C, 43.02; H, 5.11; N, 11.85; Cl, 24.11.

$[Ar_{Cl}N_2NMe]Hf(NMe_2)_2$. $Hf(NMe_2)_4$ (0.952 g, 2.68 mmol) was added to a solution of $H_2[Ar_{Cl}N_2NMe]$ (1.092 g, 2.683 mmol) in benzene (10 mL). The reaction was stirred for 16 h at room temperature. All volatile components were removed in vacuo, and the remaining solid was washed with pentane to give a yellow powder; yield 1.526 g (85%). ^1H NMR (C_6D_6): δ 2.23 (s, 3H, NCH_3), 2.34, 2.93, 3.27, and 3.93 (m, 2H each, ligand CH_2), 2.63 and 3.33 (s, 6H each, NMe_2), 6.39 (t, 2H, p-H), 7.21 (d, 4H, m-H). Anal. Calcd for $C_{21}H_{29}N_3Cl_4Hf$: C, 37.55; H, 4.35; N, 10.42; Cl, 21.11. Found: C, 37.64; H, 4.28; N, 10.36; Cl, 21.16.

$[Ar_{Cl}N_2NMe]ZrCl_2$. TMSCl (1.289 g, 11.86 mmol) was added to a solution of $[Ar_{Cl}N_2NMe]Zr(NMe_2)_2$ (1.979 g, 3.39 mmol) in toluene (25 mL) that had been cooled to −30 °C. After stirring at RT for 16 h, the reaction was concentrated in vacuo to 3 mL and 15 mL of pentane was added. A precipitate formed and was collected and washed with Et_2O and pentane to give a white powder; yield 1.375 g (72%). ^1H NMR (C_6D_6): δ 2.36 (s, 3H, NCH_3), 2.33, 2.81, 3.01, and 3.74 (m, 2H each, ligand CH_2), 6.32 (t, 2H, p-H), 6.95 (d, 4H, m-H).

$[Ar_{Cl}N_2NMe]HfCl_2$. TMSCl (2.070 g, 15.40 mmol) was added to a solution of $[Ar_{Cl}N_2NMe]Hf(NMe_2)_2$ (1.673 g, 3.081 mmol) in toluene (15 mL) that had been cooled to −30 °C. After stirring at RT for 16 h, the reaction was concentrated in vacuo to 7 mL and 5 mL of pentane was added. A precipitate formed and was collected and washed with Et_2O and pentane to give a white powder; yield 1.956 g (97%). ^1H NMR (C_6D_6): δ 2.33 (s, 3H, NCH_3), 2.28, 2.76, 3.13, and 3.92 (m, 2H each, ligand CH_2), 6.32 (t, 2H, p-H), 7.02 (d, 4H, m-H). ^{13}C NMR (C_6D_5Br): δ 45.60 (1C, NCH_3), 52.14 and 56.51 (2C each, ligand CH_2), 152.89, 129.41, 129.62, and 147.55 (12C, Ph).

$[Ar_{Cl}N_2NMe]ZrMe_2$. A solution of MeMgBr in Et_2O (0.676 mL of a 3.45 M solution, 2.33 mmol) was added via syringe to a suspension of $[Ar_{Cl}N_2NMe]ZrCl_2$ (0.630 g, 1.11 mmol) in 20 mL of Et_2O that had been cooled to −30 °C. After 1 h at room temperature, 1.0 mL of dioxane was added, which initiated the precipitation of a fine white powder. After an additional 5 min, all volatile components were removed in vacuo. The product was extracted into 25 mL of toluene. The solution was filtered through a pad of Celite and concentrated to dryness in vacuo to give a white solid; yield 0.355 g (61%). ^1H NMR (C_6D_6): δ 0.60 (s, 6H, $ZrCH_3$), 2.19 (s, 3H, NCH_3), 2.03, 2.76, 3.21, and 3.70 (m, 2H each, ligand CH_2), 6.42 (t, 2H, p-H), 7.12 (d, 4H, m-H). ^1H NMR (C_6D_5Br): δ 0.29 (s, 3H, $ZrCH_3$), 0.33 (s, 3H, $ZrCH_3$), 2.41 (s, 3H, NCH_3), 2.44, 2.99, 3.23, and 3.75 (m, 2H each, ligand CH_2), 6.65 (t, 2H, p-H), 7.17 (d, 4H, m-H). ^{13}C NMR (C_6D_5Br): δ 36.74 (1C, NCH_3), 45.32 and 46.13 (1C each, $ZrCH_3$), 53.81 and 59.83 (2C each, ligand CH_2), 125.41, 128.42, 135.71, and 146.47 (12C, Ph). Anal. Calcd for $C_{19}H_{23}N_3Cl_4Zr$: C, 43.60; H, 4.43; N, 8.03; Cl, 26.75. Found: C, 43.48; H, 4.48; N, 7.94; Cl, 26.66.

$[Ar_{Cl}N_2NMe]HfMe_2$. A solution of MeMgBr in Et_2O (0.593 mL of a 3.45 M solution, 2.05 mmol) was added via syringe to a suspension of $[Ar_{Cl}N_2NMe]HfCl_2$ (0.638 g, 0.975 mmol) in 25 mL of Et_2O that had been cooled to −30 °C. After 1 h at room temperature, 0.2 mL of dioxane was added, which completed the precipitation of a fine white powder. The reaction was worked up using a method analogous to that of $[Ar_{Cl}N_2NMe]ZrMe_2$, yielding a white solid; yield 0.465 g (77%). ^1H NMR (C_6D_6): δ 0.18 and 0.49 (s, 3H, $HfCH_3$), 2.11 (s, 3H, NCH_3), 2.04, 3.69, 3.51 and 3.52 (m, 2H each, ligand CH_2), 6.40 (t, 2H, p-H), 7.12 (d, 4H, m-H). ^1H NMR (C_6D_5Br): δ −0.13 and 0.25 (s, 3H, $HfCH_3$), 2.41 (s, 3H, NCH_3), 2.42, 2.97, 3.56, and 3.60 (m, 2H each, ligand CH_2), 6.65 (t, 2H, p-H), 7.17 (d, 4H, m-H). ^{13}C NMR (C_6D_5Br): δ 39.41 (1C, NCH_3), 53.43 and 58.28 (2C each, ligand CH_2), 55.71 and 56.50 (1C each, $HfCH_3$), 125.31, 128.40, 135.42, and 147.17 (12C, Ph). Anal. Calcd for $C_{19}H_{23}N_3Cl_4Hf$: C, 37.18; H, 3.78; N, 6.85; Cl, 23.11. Found: C, 37.26; H, 3.71; N, 6.74; Cl, 23.19.

$[Ar_{Cl}N_2NMe]Hf(i\text{-}Bu)_2$. $[Ar_{Cl}N_2NMe]HfCl_2$ (0.208 g, 0.318 mmol) was suspended in 7 mL of toluene, cooled to −30 °C, and combined with a solution of i-BuLi (0.041 g, 0.64 mmol) which had also been cooled to −30 °C. The reaction was stirred at room temperature for 1 h before all volatiles were removed in vacuo. The product was extracted into 10 mL of toluene. This solution was filtered through a pad of Celite and concentrated in vacuo to give a yellow powder; yield 0.162 g (73%). ^1H NMR (C_6D_5Br): δ 0.24 (d, 2H, i-Bu CH_2), 0.58 (d, 6H, i-Bu CH_3), 0.74 (d, 2H, i-Bu CH_2), 1.04 (d, 6H, i-Bu CH_3), 1.65 (p, 1H, i-Bu CH), 2.42 (p, 1H, i-Bu CH), 2.46 (s, 3H, NCH_3), 2.44, 2.95, 3.43, and 3.62 (m, 2H each, ligand CH_2), 6.66 (t, 2H, p-CH), 7.20 (d, 4H, m-CH). ^{13}C NMR (C_6D_5Br): δ

28.87 (2C, i-Bu CH_3), 29.28 (1C, i-Bu CH), 29.44 (2C, i-Bu CH_3), 29.74 (1C, i-Bu CH), 42.75 (1C, NCH_3), 53.18 and 59.45 (2C each, ligand CH_2), 90.00 and 91.24 (1C each, i-Bu CH_2), 125.20, 128.47, 135.26, and 148.16 (12C, Ph). Anal. Calcd for $C_{25}H_{35}N_3Cl_4Hf$: C, 43.03; H, 5.06; N, 6.02; Cl, 20.32. Found: C, 42.87; H, 5.12; N, 6.09; Cl, 20.43.

[$Ar_{Cl}N_2$NMe]HfCl(i-Bu). [$Ar_{Cl}N_2$NMe]$HfCl_2$ (0.520 g, 0.793 mmol) was suspended in 25 mL of diethyl ether and cooled to −30 °C. A diethyl ether solution (0.350 mL, 0.915 mmol) of 2.61 M (i-Bu)MgCl was cooled to −30 °C and added to the reaction, which was stirred at room temperature for 1 h. Dioxane (80 mg) was added and the reaction filtered through Celite. The filtrate was concentrated in vacuo, and the resulting pale yellow solid was washed with 10 mL of pentane and dried in vacuo; yield 0.487 g (91%). Two isomers are observed in solution: ^{1}H NMR (C_6D_6) δ 0.59 (d, 2H, i-Bu_{anti} CH_2), 0.82 (d, 2H, i-Bu_{syn} CH_2), 1.17 (d, 6H, i-Bu_{anti} CH_3), 1.26 (d, 6H, i-Bu_{syn} CH_3), 2.24 (s, 3H, NCH_3), 2.24 (s, 3H, NCH_3), 2.16, 2.71, 3.27, and 3.53 (m, 2H each, ligand CH_2 for i-Bu_{syn} isomer), 2.16, 2.71, 3.17, and 3.81 (m, 2H each, ligand CH_2 for i-Bu_{anti} isomer), 6.38 (t, 2H, p-CH), 6.38 (t, 2H, p-CH), 7.08 (d, 4H, m-CH), 7.09 (d, 4H, m-CH). Anal. Calcd for $C_{21}H_{26}N_3Cl_5Hf$: C, 37.30; H, 3.88; N, 6.21; Cl, 26.21. Found: C, 37.23; H, 3.95; N, 6.12; Cl, 26.30.

[$Ar_{Cl}N_2$NMe]Hf^{13}Me(i-Bu). [$Ar_{Cl}N_2$NMe]HfCl(i-Bu) 0.126 g, 0.187 mmol) was suspended in 10 mL of diethyl ether and cooled to −30 °C. A diethyl ether solution (0.205 mL, 0.306 mmol) of 0.8 M ^{13}MeMgCl was cooled to −30 °C and added to the reaction, which was stirred at room temperature for 1 h. Dioxane (80 mg) was added and the reaction filtered through Celite. The filtrate was concentrated in vacuo to 4 mL and stored for several days. The product precipitated as white microcrystals containing dioxane, which were collected via filtration and redissolved in toluene. The solvent was removed in vacuo to yield a white powder; yield 0.089 g (73%). [$Ar_{Cl}N_2$NMe]HfMe(i-Bu) was also synthesized using a similar method, and two isomers are observed in solution. ^{1}H NMR (C_6D_5Br): δ −0.13 (s, 3H, Me_{anti}), 0.17 (d, 2H, i-Bu_{anti} CH_2), 0.38 (s, 3H, Me_{syn}), 0.52 (d, 2H, i-Bu_{syn} CH_2), 0.76 (d, 6H, i-Bu_{anti} CH_3), 0.95 (d, 6H, i-Bu_{syn} CH_3), 1.52 (m, 1H, i-Bu_{anti} CH), 2.23 (m, 1H, i-Bu_{syn} CH), 2.41 (s, 3H, NCH_3), 2.45 (s, 3H, NCH_3), 2.48, 3.00, 3.57, and 3.61 (m, 2H each, ligand CH_2 for i-Bu_{syn} isomer), 2.48, 3.00, 3.45, and 3.70 (m, 2H each, ligand CH_2 for i-Bu_{anti} isomer), 6.64 (t, 2H, p-CH), 6.65 (t, 2H, p-CH), 7.12 (d, 4H, m-CH), 7.14 (d, 4H, m-CH). ^{13}C NMR (C_6D_5Br): δ 28.48 (1C, i-Bu_{syn} CH), 28.85, (2C, i-Bu_{anti} CH_3), 28.88 (1C, i-Bu_{anti} CH), 29.16 (2C, i-Bu_{syn} CH_3), 41.33 (1C, NCH_3 for i-Bu_{syn} isomer), 41.91 (1C, NCH_3 for i-Bu_{anti} isomer), 53.06 and 57.29 (2C each, ligand CH_2 for i-Bu_{syn} isomer), 53.26 and 56.92 (2C each, ligand CH_2 for i-Bu_{anti} isomer), 56.01 (1C, $CH_{3\ syn}$), 58.19 (1C, $CH_{3\ anti}$), 86.99 (1C, i-Bu_{syn} CH_2), 89.60 (1C, i-Bu_{anti} CH_2), 125.18, 128.36, 135.21, and 147.73 (12C, Ph for i-Bu_{anti} isomer), 125.22, 128.36, 135.42, and 147.57 (12C, Ph for i-Bu_{syn} isomer). ^{13}C NMR ($C_6D_5CD_3$): δ 56.38 (1C, $^{13}Me_{syn}$), 59.19 (1C, $^{13}Me_{anti}$). Anal. Calcd for $C_{22}H_{29}N_3Cl_4Hf$: C, 40.29; H, 4.46; N, 6.41; Cl, 21.62. Found: C, 40.21; H, 4.38; N, 6.50; Cl, 21.54.

The Me_{anti} → Me_{syn} isomerization process in [$Ar_{Cl}N_2$NMe]-Hf(i-Bu)Me was studied by observing the disappearance of the Me_{anti} ^{1}H NMR resonance and the growth of the Me_{syn} resonance in relation to a known Ph_3CH standard. Thermodynamic parameters were calculated by employing Van't Hoff and Eyring plots. The data are the following: T = 50 °C, K = 1.10, k_1 = 0.000593 s^{-1}; 60 °C, 1.13, 0.00136 s^{-1}; 65 °C, 1.15, 0.00268 s^{-1}; 70 °C, 1.16, 0.00425 s^{-1}; 75 °C, 1.18, 0.00699 s^{-1}; 80 °C, 1.20, 0.0990 s^{-1}.

General Procedure for Activation of [$Ar_{Cl}N_2$NMe]MR_2 (M = Hf, Zr). Solutions of [$Ar_{Cl}N_2$NMe]MR_2 (0.003−0.012 mmol; 1 equiv) and {Ph_3C}{$B(C_6F_5)_4$} (0.003−0.012 mmol; 1 equiv), $B(C_6F_5)_3$ (0.003−0.012 mmol; 1 equiv), or {$HNMe_2Ph$}-{$B(C_6F_5)_4$} (0.003−0.012 mmol; 1 equiv) and the internal standard Ph_2CH_2 (0.048 mmol) in C_6D_5Br (X, Y = (1.0 − X − H) mL, respectively; H = volume of 1-hexene to be added later in polymerization reactions only) were cooled to −30 °C and mixed. Activation was almost immediate for the {Ph_3C}-{$B(C_6F_5)_4$}, $B(C_6F_5)_3$, and {$PhNMe_2H$}{$B(C_6F_5)_4$} activators and accompanied by a change in color of the solution from deep orange to yellow when {Ph_3C}{$B(C_6F_5)_4$} was the activator. The reaction was transferred to an NMR tube, which was frozen in liquid nitrogen, and the solution was thawed to 0 °C at time = 0.

General Procedure for Polymerization Reactions. [$Ar_{Cl}N_2$NMe]MR_2 (M = Hf, Zr) was activated as described previously, and 1-hexene (50−500 equiv) was immediately added to the vigorously stirred, cooled (−30 °C) solution. The reaction was transferred to an NMR tube, which was frozen in liquid nitrogen and then thawed in the NMR probe at 0 °C. Upon complete consumption of 1-hexene, the reactions were quenched with methanol. After solvent removal, the polymer was dissolved in pentane and the solution filtered through silica gel. The solvent was removed in vacuo to give poly[1-hexene] in 100% yield.

{[$Ar_{Cl}N_2$NMe]ZrMe}{$B(C_6F_5)_4$}. ^{1}H NMR (0 °C, C_6D_5Br): δ 0.62 (s, 3H, $HfCH_3$), 2.34 (s, 3H, NCH_3), 2.65, 2.91, 3.76, and 3.83 (m, 2H each, ligand CH_2), 6.50 (t, 2H, p-H), 6.96 (d, 4H, m-H).

{[$Ar_{Cl}N_2$NMe]HfMe}{$B(C_6F_5)_4$}. ^{1}H NMR (0 °C, C_6D_5Br): δ 0.49 (s, 3H, $HfCH_3$), 2.36 (s, 3H, NCH_3), 2.62, 2.95, 3.80, and 3.90 (m, 2H each, ligand CH_2), 6.57 (t, 2H, p-H), 6.96 (d, 4H, m-H).

{[$Ar_{Cl}N_2$NMe]HfMe}{$MeB(C_6F_5)_3$}. ^{1}H NMR (20 °C, C_6D_5Br): δ 0.80 (s, 3H, $HfCH_3$), 1.12 ($MeB(C_6F_5)_3$) 2.41 (s, 3H, NCH_3), 2.86, 2.23, 3.62, and 3.90 (m, 2H each, ligand CH_2), 6.62 (t, 2H, p-H), 7.18 (d, 4H, m-H).

{[$Ar_{Cl}N_2$NMe]HfMe(NMe_2Ph)}{$B(C_6F_5)_4$}. ^{1}H NMR (0 °C, C_6D_5Br): δ 0.18 (v br s, 3H, $HfCH_3$), 2.39 (s, 3H, NCH_3), 2.45 (m, 2H, ligand CH_2), 2.58 (s, 6H, NMe_2Ph), 2.95 and 3.46 (br s, 2H each, ligand CH_2), 3.30 (v br s, 2H, ligand CH_2), 6.72 (t, 2H, p-H), 7.19 (d, 4H, m-H), 6.0−7.2 ppm (5H, NMe_2Ph aryl H's).

{[$Ar_{Cl}N_2$NMe]Hf(i-Bu)}{$B(C_6F_5)_4$}. ^{1}H NMR (0 °C, C_6D_5Br): δ 0.92 (br s, 6H, i-Bu CH_3), 0.95 (br s, 2H, i-Bu CH_2), 2.55 (s, 3H, NCH_3), 2.55 (br s, 1H, i-Bu CH), 2.62, 3.07, 3.76, and 3.86 (m, 2H each, ligand CH_2), 6.53 to 7.20 (aryl H's).

{[$Ar_{Cl}N_2$NMe]Hf(i-Bu)}{$HB(C_6F_5)_3$}. ^{1}H NMR (0 °C, C_6D_5Br): δ 0.91 (br s, 6H, i-Bu CH_3), 0.96 (br s, 2H, i-Bu CH_2), 2.58 (s, 3H, NCH_3), 2.58 (br s, 1H, i-Bu CH), 2.66 and 3.10 and 3.71 and 3.81 (m, 2H each, ligand CH_2), 6.55 (t, 2H, p-H), 6.95 (d, 4H, m-H). ^{1}H NMR (0 °C, $C_6D_5CD_3$): δ 0.88 (d, 6H, i-Bu CH_3), 1.02 (d, 2H, i-Bu CH_2), 2.39 (s, 3H, NCH_3), 2.39 (p, 1H, i-Bu CH), 2.88, 2.92, 3.49, and 3.54 (m, 2H each, m, ligand CH_2), 6.35 (t, 2H, p-H), 6.82 (d, 4H, m-H).

{[$Ar_{Cl}N_2$NMe]Hf(C_8H_{17})}{$HB(C_6F_5)_3$} (isobutyl 1,2 insertion product). ^{1}H NMR (0 °C, C_6D_5Br): δ 0.57 (d, 6H, CH_3), 0.81 (s, 6H, CH_3) 0.91 (d, 2H, CH_2), 1.16 (s, 2H, CH_2), 1.26 (p, 1H, CH), 2.60 (s, 3H, NCH_3), 2.71, 3.11, 3.72, and 4.03 (m, 2H each, ligand CH_2), 6.56 (t, 2H, p-H), 6.96 (d, 4H, m-H).

Asymmetric Product of the Reaction of {[$Ar_{Cl}N_2$NMe]-Hf(i-Bu)}{$B(C_6F_5)_4$} with Dimethylaniline and {$HNMe_2Ph$}{$B(C_6F_5)_4$} Activation of {[$Ar_{Cl}N_2$NMe]Hf(i-Bu)$_2$}. ^{1}H NMR (20 °C): δ 1.48 (s, 3H), 2.46 (s, 3H), 2.58 (s, 3H), 2.18, 2.31, 2.60, 3.20, 3.26, 3.34, 3.68, 4.32, 4.51 (m, 1H each), 2.90 and 3.20 (dd, 2H), 3.16 (d, 1H), 5.85 (t, 1H), 6.59 (d, 2H), 6.62 and 6.72 (t, 1H each, m-H), 6.78−6.86 (m, 2H), 7.05 (d, 2H), 7.08−7.20 (m).

Acknowledgment. We thank the Department of Energy (DE-FG02-86ER13564) for supporting this research.

Supporting Information Available: Fully labeled thermal ellipsoid drawing, crystal data and structure refinement, atomic coordinates, bond lengths and angles, anisotropic displacement parameters, and hydrogen coordinates for [(2,6-$Cl_2C_6H_3NCH_2CH_2)_2$NMe]Hf(i-Bu)$_2$. This material is available free of charge via the Internet at http://pubs.acs.org. Details of the structure of [(2,6-$Cl_2C_6H_3NCH_2CH_2)_2$NMe]$HfMe_2$ can be found in the preliminary communication.[28]

OM040113H